SAE *International*®

A Next Generation Cordierite Diesel Particle Filter with Significantly Reduced Pressure Drop

Thorsten Boger, Suhao He, Thomas Collins, Achim Heibel, Douglas Beall and Christophe Remy
Corning Inc.

ABSTRACT

Diesel particle filters (DPF) have become a standard after treatment component for all current and future on-road diesel engines used in the US. In Europe the introduction of EUVI is expected to also result in the broad implementation of DPF's. The anticipated general trend in engine technology towards higher engine out NOx/PM ratios results in a somewhat changing set of boundary conditions for the DPF predominantly enabling passive regeneration of the DPF. This enables the design of a novel filter concept optimized for low pressure drop, low thermal mass for optimized regeneration and fast heat-up of a downstream SCR system, therefore reducing CO_2 implications for the DPF operation. In this paper we will discuss results from a next generation cordierite DPF designed to address these future needs. The new materials are based on a thinwall design with optimized material and microstructure, resulting in an almost linear pressure drop response with soot loading in the bare and catalyzed state. A significant reduction in soot loaded pressure drop for uncoated and coated filters is demonstrated of the new filter design vs. current EPA 2010 filter technologies. The optimized microstructure also enables high filtration efficiency for mass and number. Results from a wide range of regeneration experiments will be used to discuss the thermal operating window of the new material and the thermal response during normal operation and active regeneration. A uniform temperature distribution and the fast thermal response of the low mass filter minimize implications on fuel consumption.

INTRODUCTION

Diesel particulate filters have been used for several decades in retrofit and certain particulate emissions focused applications. With the introduction of EPA 2007 regulations, diesel particulate filters became the standard choice of technology for meeting emissions requirements for on-road vehicles in the US and Canada. These systems were implemented with a combination of active and passive regeneration, where the lack of DeNOx aftertreatment resulted in a reduced range for optimum passive regeneration operation. To comply with the strict NOx emissions limits (0.2 g/(hp·hr)) in EPA 2010 many systems implemented SCR based DeNOx technology (Figure 1).

This also enabled engine makers to take advantage of lower fuel consumption by calibrating for lower engine out PM and higher NOx emissions and furthermore widened the window for passive regeneration operation. A similar direction is anticipated for systems complying with EUVI regulations, as the regulated tailpipe NOx emissions levels are significantly higher allowing higher engine-out NOx emissions at similar DeNOx efficiencies.

With higher engine-out NOx/PM ratios the filter requirements change as the hydrodynamic, filtration and thermal aspects gain importance with predominantly passive regeneration operation focused systems. It is anticipated that next generation DPF designs need to be as fuel consumption neutral as possible by providing ultra low restriction and supporting engine thermal management needs in cold start and regeneration operations.

Future directions to reduce fuel consumption to meet anticipated CO_2 or GHG emissions limits and also reduce operating cost for the end user, especially given the potential for higher fuel prices, support this direction.

PRODUCT CONCEPT

As outlined in the previous section, new designs and products are based on the assumption of a need for 1) reduced pressure drop with improved deep bed filtration impact related to the soot loaded pressure drop, 2) reduced thermal mass for optimized regeneration and fast heat-up of a downstream SCR system, and 3) decreased soot mass limit requirements due to the expected trend towards engines operating at higher
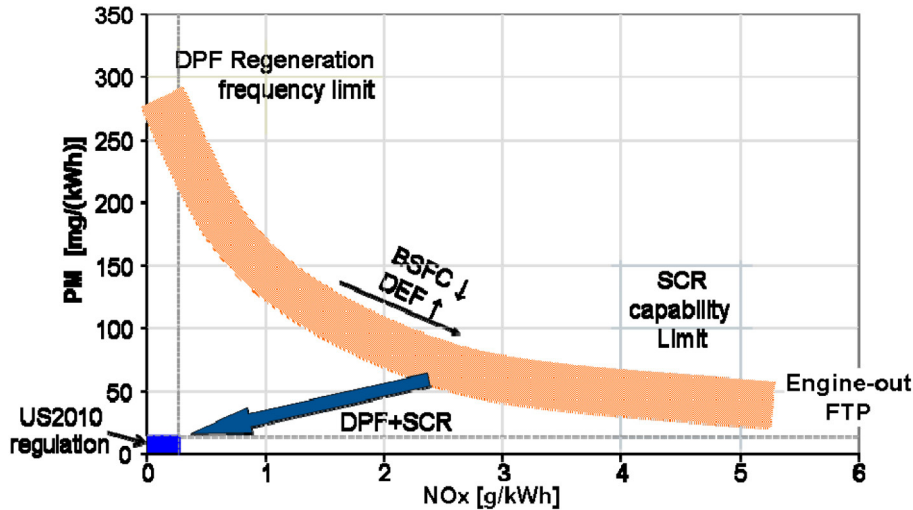
Figure 1. NOx/PM engine-out trade-off for modern heavy duty diesel engine

NOx/PM ratios. Alternatively the reduced pressure drop could be used to enable more compact filters, which might be especially attractive in cases where packaging space is limited. All features target enhanced fuel efficiency and reduced CO_2 emissions. To achieve the development goals a new family of cordierite materials has been developed that provides a significantly widened window with respect to new cell designs combined with a highly engineered microstructure that minimizes the impact of soot on permeability and pressure drop.
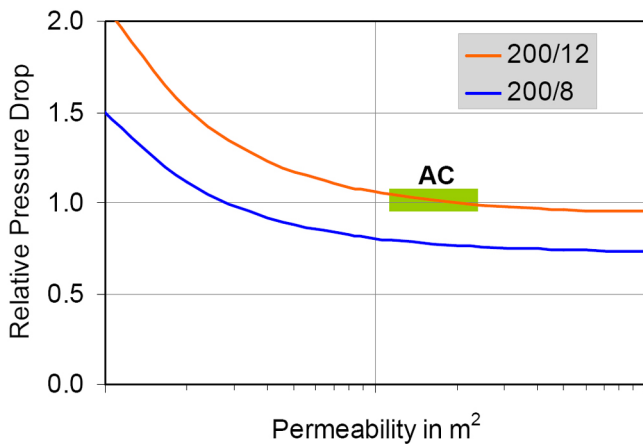

Figure 2. Relationship between filter pressure drop and permeability.

When looking for opportunities to further reduce the pressure drop of particulate filters, it is instructive to evaluate the relationship between pressure drop and permeability. The latter is the property describing the impact of the material and microstructure on the filter pressure drop. An example of this relationship is shown in Figure 2. Plotted is the relative pressure drop as a function of the wall permeability. The

pressure drop has been normalized to values typical for DuraTrap® AC for conditions without soot (i.e. clean). Starting with the data for the 200cpsi/12 mil (0.012inch) cell geometry one can see that for advanced materials with high permeability (assuming no soot present), such as DuraTrap® AC, the pressure drop is only a weak function of the permeability and a further improvement would provide limited benefit. The pressure drop is primarily determined by the cell geometry. A reduction in web thickness will provide a significant reduction in pressure drop, as can be seen from Figure 2 for the example of a reduction from 12mil to 8mil.

Another consideration for particulate filter design and operation is the impact of soot on the pressure drop response. In general soot that accumulates inside the pores of the filter walls reduces overall permeability, leading to a higher pressure drop. Unlike the clean pressure drop discussed in the previous paragraph, this effect is a strong function of the design of the filter microstructure material. Although significant achievements were made during the development of products for EPA 2010, resulting in advanced filter products such as DuraTrap® AC [1], our next generation cordierite filters offer an even further improved microstructure with an increased porosity of ~55-57% and a highly engineered pore size distribution. The mean pore size has been reduced compared to DuraTrap® AC and the pore size distribution has been further tightened and tailored. As will be shown in the following sections, this new microstructure significantly reduces the effect of deep bed penetration of soot, yielding a soot loaded pressure drop which can range from 30-50% lower than with current EPA 2010 products.

The accumulation of ash and its impact on the evolution of the pressure drop during the life of a filter is a critical aspect considered during the design of a filter, which is primarily driven by the cell geometry and, eventually, the size of the

filter. Comparing filters in 200/12 and 200/8 cell geometries, one finds a roughly 14-15% increased inlet volume available for storage of ash due to the thinner webs. This difference, combined with the lower pressure drop, could be used to enable lower pressure drop throughout the filter life or to trade some of the pressure drop reduction for a reduced filter size while maintaining ash capacity. The latter concept can be used to an even larger extent if alternative cell designs are considered, involving higher cell densities that increase the specific filtration area per volume as well as asymmetric cell design such as the ACT technology described in reference [2-3]. An especially attractive option utilizing the features described above combined with the improved microstructure is 300/7 ACT design. As will be shown in the following sections, this filter allows for the most compact design at pressure drop comparable to the current EPA 2010 products.

The new filter product utilizes designs with reduced web thickness, reducing the total volume fraction represented by the honeycomb walls. In addition, it was mentioned that the new microstructure offers an increased porosity, which further reduces the overall solid fraction of the filter. To compensate, the new filter is based on a new family of cordierite materials that provide increased intrinsic material strength, allowing the strength of the honeycomb structure to be comparable to the strength of current filter products in a 200/12 geometry.

In the following sections experimental results obtained with the new cordierite material in 200/8 and 300/7 ACT cell geometries, or thin wall filter (TWF) geometries, will be discussed to demonstrate the target benefits described above.

PRESSURE DROP

Pressure drop testing was performed on 200/8 and 300/7 ACT filter cell geometries with the filters being of varying lengths. The engine used for pressure drop testing is a 9L 6-cylinder engine with EPA 2007 calibration. The pressure drop test [3] contains a variety of engine conditions and results are normalized to a standard flow rate and temperature condition. Since the samples had different volumes, the testing was performed in a manner to enable comparison of pressure drop at equivalent soot levels, i.e., grams of soot loaded, regardless of the filter volume. Figure 3 shows the clean and soot loaded pressure drop, in two different formats. The first graph, 3(a) shows pressure drop as a function of soot per liter of filter. The TWFs show a significantly reduced pressure drop in comparison to the 2007 and 2010 technology references. The lowest pressure drop is from the TWF $\varnothing 10''\times 11''$ in 200/8 geometry. The second graph 3(b) shows pressure drop as a function of grams of soot on the filters, which demonstrates how any of the filters will perform if placed into an application with a consistent soot load to regeneration. In this case, the $\varnothing$ $10''\times 11''$ TWF 200/8 still performs the best. Deep bed filtration effects, defined by the sharp increase in pressure drop at initial soot loading stage, are much smaller for TWF products than 2007 and 2010 (AC) technology references. The improvement is achieved through an even further improved microstructure with an increased porosity of ~55-57% and a highly engineered pore size distribution. It can also be noted that the pressure drop difference between bare and coated product is minimal. The minimal wash-coat impact may be different with alternate wash-coat loadings and catalyst technologies.
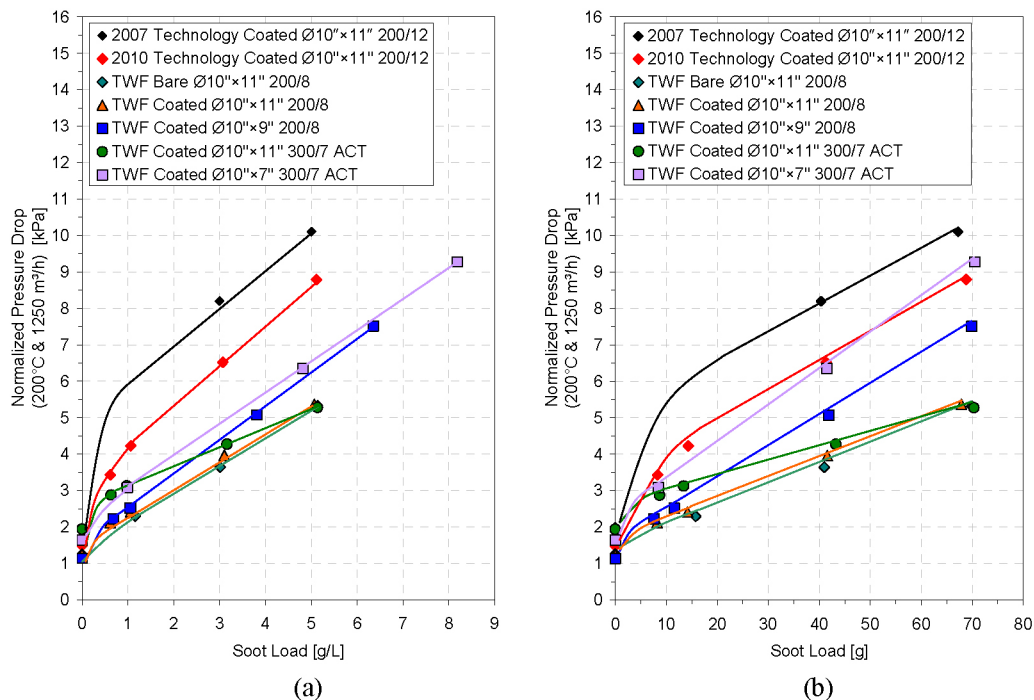

(a)

(b)

Figure 3. Comparison of pressure drop a) as a function of grams of soot per liter of filter and b) as a function of grams of soot
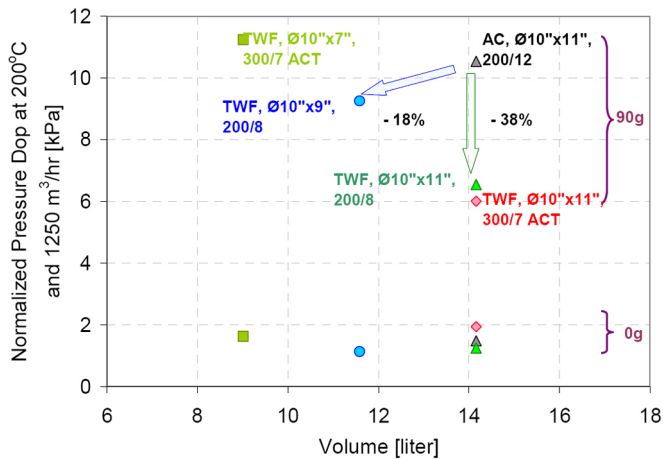
Figure 4. Improvement on either pressure drop or volume for coated TWF versus coated AC filters. The two sets of data represent different soot loads (clean 0g and 90g).

Figure 4 shows how thin wall designs can be utilized for enhanced after-treatment integration by either reducing pressure drop or reducing filter volume. For example, comparing the change from AC 200/12 in $\varnothing 10''\times11''$ to TWF 200/8 in $\varnothing 10''\times11''$, a roughly 40% reduction in pressure drop can be achieved. Alternatively, selecting the alternative of TWF 200/8 in $\varnothing 10''\times9''$ would enable a roughly 20% reduction in pressure drop combined with approximately 20% reduction in volume. Similar benefits in terms of either lower pressure drop at given volume or significantly reduced volume at comparable pressure drop can be achieved when the design with higher cell density, 300/7, is utilized combined with the asymmetric cell technology (ACT) for enhanced ash storage. In general, due to the thin wall design, the TWF is expected to have much more volume for ash storage for the same filter volume, for example, about 15% increase ash storage from 200/12 to 200/8, or roughly 45% from 200/12 to 300/7 ACT. Therefore, an even lower pressure drop is expected over the life time of the filter.
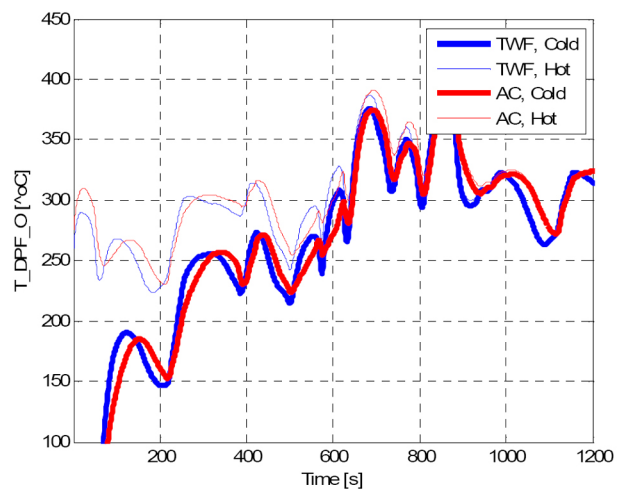
THERMAL RESPONSE

COLD START

Cold and hot FTP tests were ran with $\varnothing 10''\times11''$ coated TWF 200/8 and $\varnothing 10''\times11''$ coated AC 200/12 filters. From Figure 5, filter inlet temperature is identical for the compared cases. For the cold cycle experiments, engine and after-treatment compartments are cooled down to room temperature before the start of the test. The outlet temperature profiles shown in Figure 5b demonstrate that the TWF has a much faster thermal response compared to the AC reference filter. This holds for both the heat-up and the cool-down curves, and is explained by the ~45% lower thermal mass of the filter. The same reduction in thermal mass of ~45% is obtained for the other TWF cell configuration, 300/7 ACT, when compared at equal filter volume.

The accumulated density of the DPF outlet temperature is compared in Figure 6. Only the data from the first 400 seconds of the cold start cycle are used, as these represent the time frame of prime interest. For example, for AC filter outlet temperature during the cold cycle, the accumulated density is 0.6 at 185°C, which means for 60% of the 400 seconds, temperature is below 185°C. It should be mentioned that the benefits of an extended temperature window due to low thermal mass are expected to strongly depend on the test cycle and the application. For the FTP cycle shown in Figure 6, and systems in which the downstream SCR catalyst starts operating
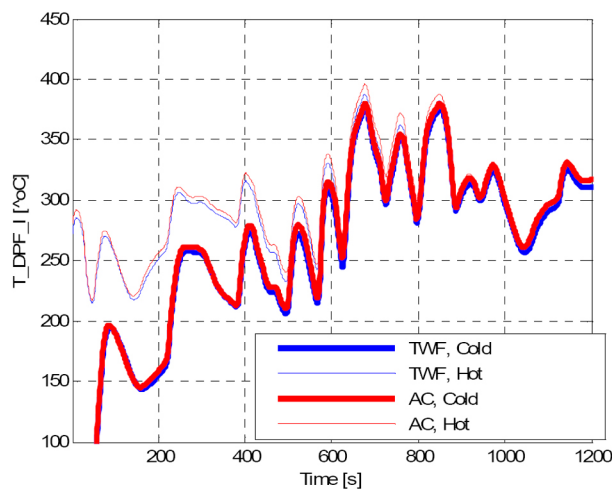
(a)

(b)

Figure 5. Comparison of thermal response during cold and hot FTP test performed on $\varnothing$ 10"×11" 200/8 coated TWF and $\varnothing$ 10"×11" 200/12 coated AC filters: a) DPF inlet temperature; b) DPF outlet temperature.
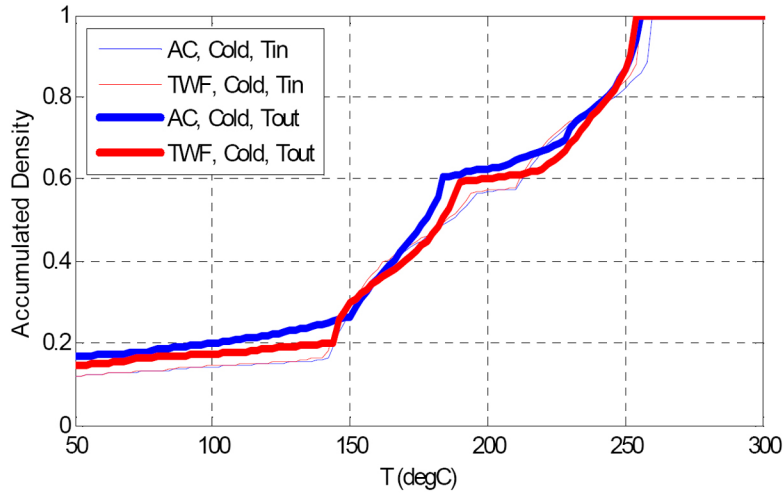
Figure 6. Comparison of accumulated DPF outlet temperature distribution for the first 400 seconds of cold and hot FTP tests performed on coated TWF and coated AC filters.

at 180°C, the TWF extends the operating window by 6% (or 24 sec), which can be of relevance with respect to the overall NOx conversion given that a significant portion of the emissions are due to the low temperature regime. Further benefits can be expected for a system design with reduced filter volume. It is
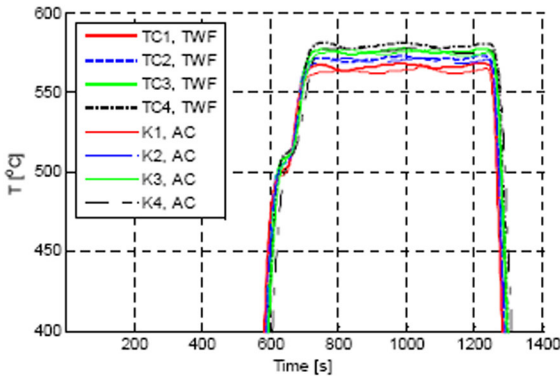
also expected that the lower thermal mass of the TWF will enable an increased NO_2 generation over an oxidation catalyst applied onto it due to the extended temperature window. This will be of practical relevance for both passive regeneration of soot inside the filter and the downstream SCR performance.
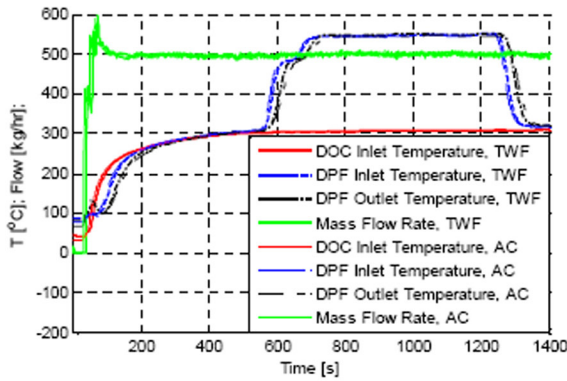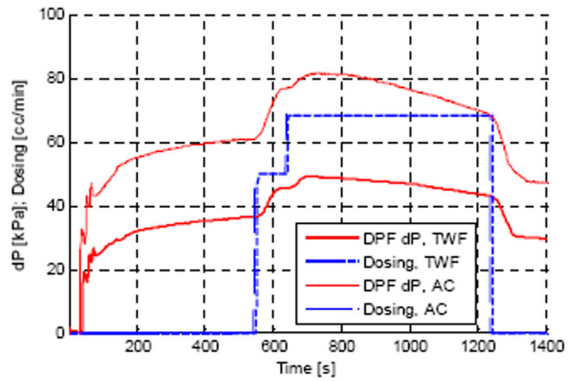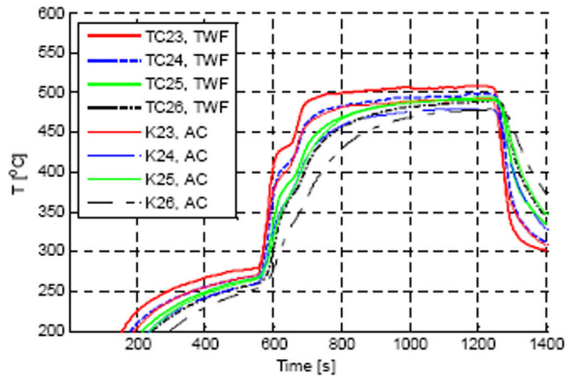

Figure 7. Comparison of controlled regeneration test conditions and thermal response between ⌀ 10"×11" coated TWF 200/8 and ⌀ 10"×11" coated AC 200/12: a) temperature and flow rate; b) pressure drop and hydrocarbon dosing; c) DPF bed temperature along center line; d) DPF bed temperature along skin line.
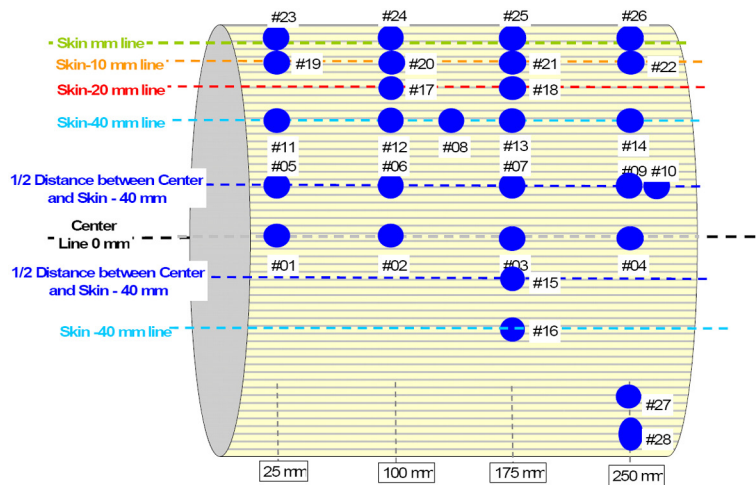
Figure 8. DPF thermocouple build.

CONTROLLED REGENERATION

Controlled regeneration tests were run on coated TWF 200/8 and coated AC 200/12 filters, both $\varnothing 10''\times 11''$, at the same engine point, with 300°C DOC inlet temperature and 500 kg/hr exhaust mass flow. In both cases, an equal initial DPF soot load of 5 g/l and variable external hydrocarbon dosing quantities were used. Test conditions are shown in Figure 7. When the engine was stabilized after around 10 minutes, fuel was dosed through an external doser installed upstream of the DOC. The dosing was performed in two stages, 3 liters/hour for 90 seconds and then at different set points of 4.1, 4.5, 4.9, 5.3, and 5.7 liters/hour for 10 minutes to simulate a staged regeneration. Thermocouples were inserted into the filters from the outlet channels to measure the DPF bed temperature, with locations illustrated in Figure 8. After each test, the filter was weighed to determine the regeneration efficiency followed by a clean out regeneration step.
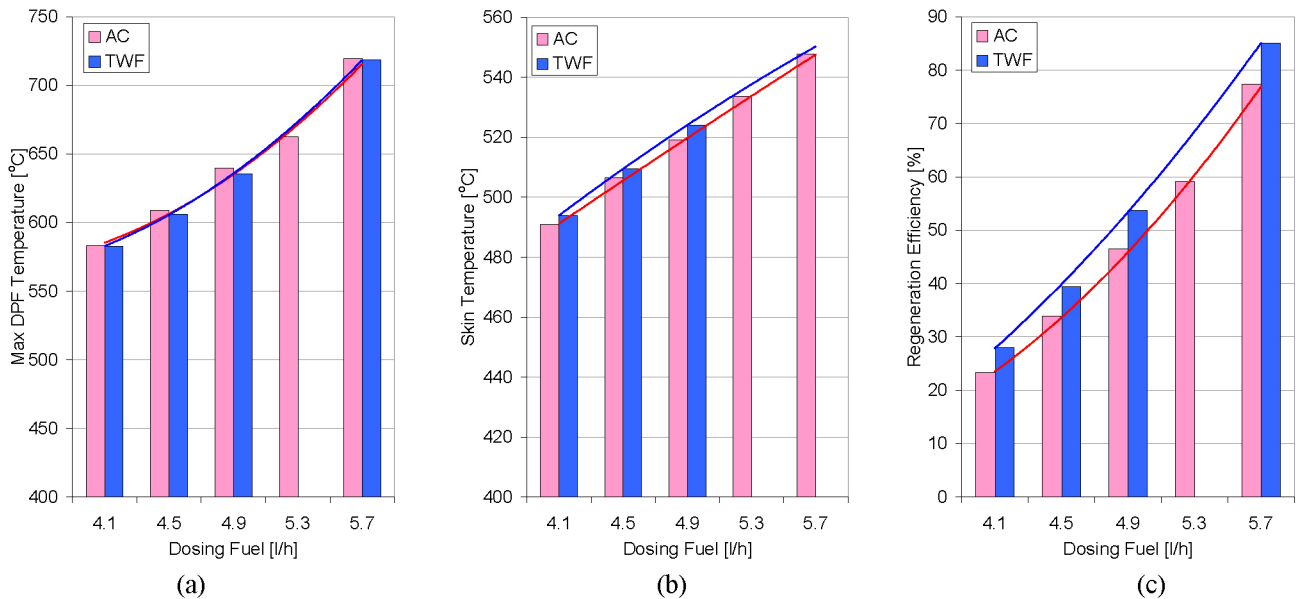

(a)   (b)   (c)

Figure 9. Comparison of a) max DPF temperature, b) skin temperature, and c) regeneration efficiency as a function of dosing rate between coated AC and coated TWF.

The thermal response of the TWF is quite different compared to AC, mostly due to the significantly reduced thermal mass. This can be seen by looking at the data from the thermocouples TC1 through TC4, located in filter centerline, and thermocouples TC23 through TC26, located along the filter skin, as shown in Figure 7 c and d. Along the centerline, the temperature response is very similar for both filter types since the convective heat transfer is balanced by the heat release. At the filter inlet, the TWF shows a slightly higher bed temperature, likely due to more effective local heat transfer. Along the filter skin line, convective heat transfer is not as significant as in the center due to less available heat from exhaust and radial heat dissipation. As a result, the heat storage term becomes important and the TWF shows faster heat-up due to its lower thermal mass. With a similar rationale the differences in steady state bed temperature can be explained.

Data at the various dosing rates considered are summarized in Figure 9. Overall, under the same controlled regeneration conditions, the TWF has similar maximum bed temperature as AC, but higher front and peripheral bed temperature. This is due to a faster heat up and a more effective local heat transfer. Both improve the overall regeneration efficiency achieved under the given sets of operation (Figure 9c).

UNCONTROLLED REGENERATION

Uncontrolled regeneration or drop-to-idle tests were performed on both coated TWF 200/8 and coated AC 200/12 filters, both in ∅10″×11″. Mass flow rate before the drop-to-idle was 750

kg/hr and 220kg/hr for idle condition. Hydrocarbon fuel was dosed before the DOC to raise DPF inlet temperature and achieve different target temperatures of 540, 560, 580 and 600°C, with a staged regeneration strategy applied. Dosing rate was set to zero once a drop-to-idle event is triggered. The drop-to-idle trigger used for this study was a combined one, based either on the bed temperature (TC2) exceeding 650°C or the pressure drop across DPF decreasing by 1.5 mbar after reaching the peak point. Thermocouples were inserted into the filters from outlet channels to measure DPF bed temperature, with the same thermocouple build as illustrated in Figure 8. Prior to the regeneration experiments the DPFs were preloaded to different target soot loads of 3, 4, 5 and 6 g/l. Analogous to the procedure for controlled regeneration, the filters were weighed after the drop to idle regeneration to determine the regeneration efficiency.

Figure 10 shows summarized data for uncontrolled regeneration tests. Figure 10a shows the maximum temperatures observed inside the filter and Figure 10b shows the fraction of soot that was oxidized during the uncontrolled regeneration event. It should be noted that these regeneration efficiencies are low since the aim of the experiment is to simulate a regeneration which is interrupted shortly after its initiation, creating a worst case thermal condition. As can be seen from the data shown, and as expected, the amount of soot oxidized is higher when the initial soot load or the inlet temperature is higher. In Figure 10a the solid lines show the trend of the response for the TWF at various soot loads. The dotted lines show results for

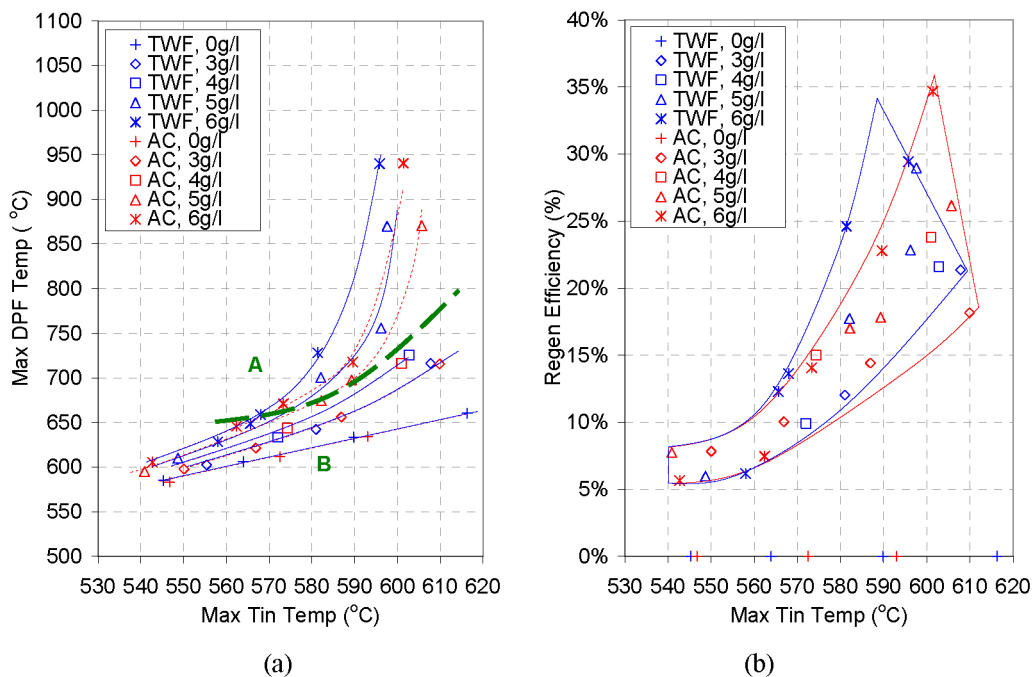(a)   (b)

Figure 10. a) Max DPF bed temperature and b) regeneration efficiency as a function of max DPF inlet temperature for uncontrolled regeneration tests with coated AC and coated TWF filters at various soot loads.

the AC filter. Under conditions of low soot load or low inlet temperatures, TWF and AC have the same response. This regime is marked as zone B below the bold dashed line. In zone B, the convective heat transfer is balanced with heat generation from the oxidation of soot, similar to what was discussed for the controlled regeneration data in the previous section. Heat storage, which is more dependent on material, is of less relevance compared to the convective term and the source term. In zone A, with conditions above the bold dashed line, local effects are more important. Under these conditions the convective heat transfer is not sufficient to remove the heat released at a sufficient rate. As a result, the local bed temperature increases sharply and the soot load drops quickly. Under these conditions, the maximum local temperature is a function of the local thermal mass, representing the ability of the filter to absorb heat. This can be seen in the higher temperatures observed with the TWF, shown in Figure 10a. It is interesting to note that the regeneration efficiencies, plotted in Figure 10b vs. the maximum DPF inlet temperatures, show no distinction between zone A and zone B. TWF in general has a higher regeneration efficiency compared to AC.

The mid-bed temperature is defined in the filter center, 2~4 centimeters from the skin, including TC13, TC16, and TC18, as shown in Figure 8. In Figure 11a it is shown that in all the uncontrolled regeneration tests, the TWF has the same maximum mid-bed temperature as AC, which indicates that under the test conditions used, in the mid-bed area, the heat release is balanced with convective heat transfer. In other words, no runaway conditions occur in this area. Figure 11b

shows that the TWF enables higher skin temperatures than AC, indicated by data measured at TC24 and TC25 shown in Figure 8. Since the thermal stress in a DPF is correlated to the temperature difference between mid-bed and skin, lower thermal stresses are expected for TWF filter. This is confirmed by stress calculations and results are shown in Figure 11c. The thermal exposure parameter is derived by first applying a numerical stress model with the experimental temperature field, and then normalizing the maximum thermo-mechanical stress by a reference value.

FILTRATION EFFICIENCY

Filtration tests for mass and number were performed on a heavy duty engine. Figure 12 shows PM measurement during the above FTP test for coated TWF 200/8 in $\varnothing 10'' \times 11''$. Filters were cleaned out first and preconditioned with 20 minutes rated power before cold and hot FTP cycles. DPF outlet PM is well below 2010 EPA heavy duty regulation limit, 0.0134g/kw.hr.

Alternate PMP testing was performed using WHTC cycle on $\varnothing 12'' \times 11''$ coated TWF 200/8 filters. In the measurements the PMP protocol [4] was followed, which requires the filter to be cleaned, conditioned with a small amount of soot and then cold soaked for a minimum of 8 hours at room temperature before testing. Composite weighted (14% cold start and 86% hot start) particle number can be found in Figure 13. For this engine and after-treatment configuration the TWF performs well below proposed EUVI limit, 6E11 #/kw.hr.
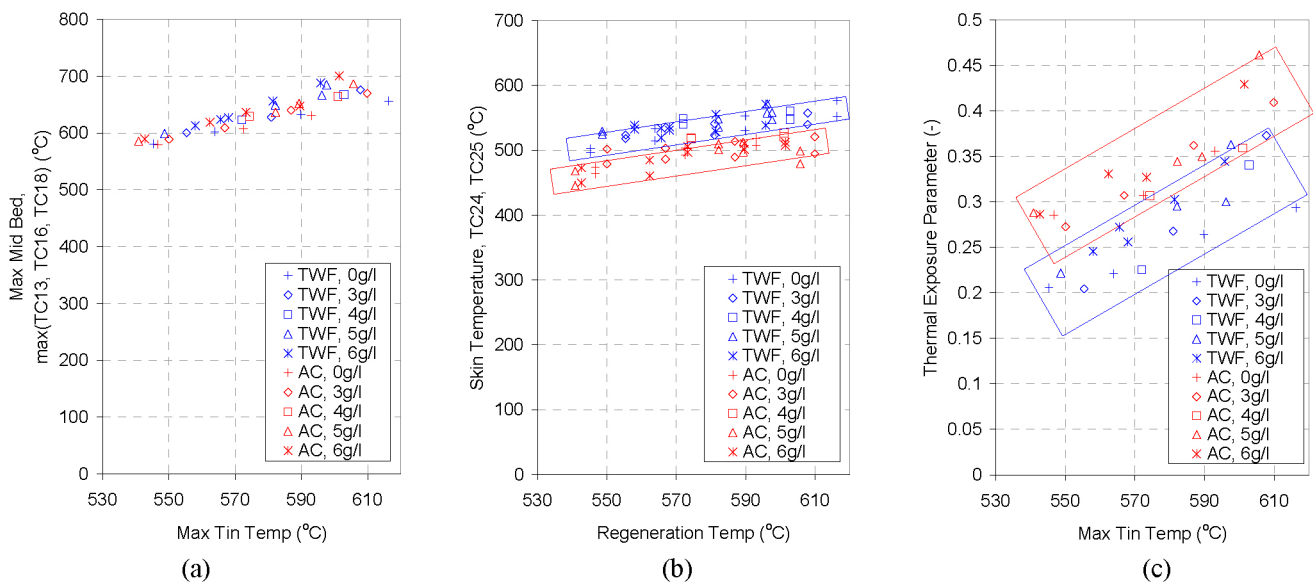

Figure 11. a) Max mid-bed temperature (TC13, TC16, and TC18), b) skin temperature (TC24 and TC25), and c) thermal exposure parameter as a function of max DPF inlet temperature during uncontrolled regeneration tests with coated AC and coated TWF filters at various soot loads.
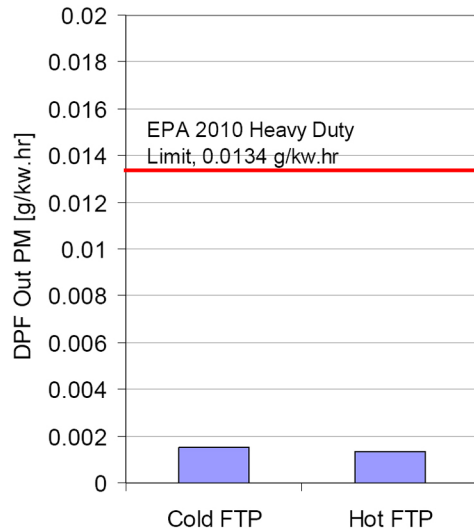
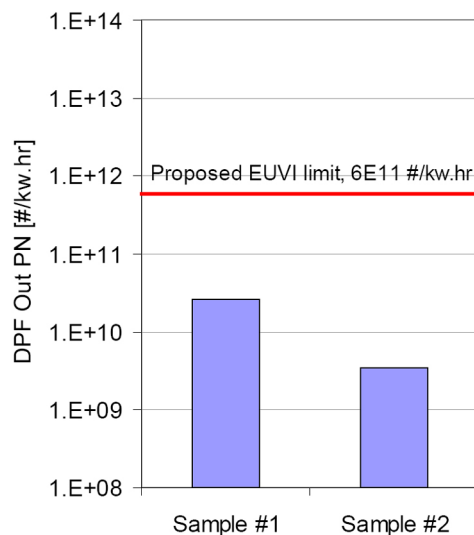**Figure 12. FTP filtration performance of $\varnothing$ 10″×11″ coated TWF 200/8.**

Figure 13. Composite weighted PN # from WHTC Tests for $\varnothing$ 12″×11″ 200/8 coated TWF following PMP Protocol.

SURVIVABILITY

Uncontrolled regeneration (or drop to idle) tests were also performed on both bare AC 200/12 and bare and catalyzed TWF filters in a 200/8 configuration ($\varnothing$12″×11″), but with a higher inlet temperature 650°C and lower idle flows. The intent of the testing was to induce a higher stress on the samples and determine the thermal operating window for the TWF product. By incrementally increasing the soot loads between tests, the maximum gradients and thermal stress increases until the samples fail. In these experiments the failure was defined by internal cracking. It should be mentioned that at this criterion the filtration function was generally not or only
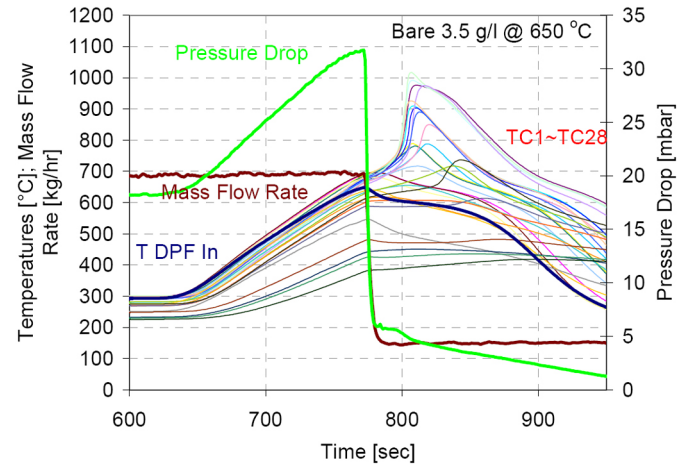

Figure 14. Engine conditions for uncontrolled regeneration tests performed on $\varnothing$ 12″×11″ filters.

slightly impacted. Test conditions are shown in Figure 14. Mass flow rate was 680 kg/hr before drop-to-idle and 150kg/hr for idle condition. Hydrocarbon fuel was dosed before the DOC to raise the DPF inlet temperature to target temperature and set to zero when a drop-to-idle event was triggered. The trigger used for this study was bed temperature (TC2, see Figure 8) over 680°C. The same procedures as for controlled regenerations were followed for thermocouple placement and weighing for regeneration efficiencies.

The TWF does demonstrate acceptable radial gradient response. Both radial gradients and thermal exposure parameter versus maximum bed temperature are shown in Figure 15. Similar to thermal exposure parameter, radial gradient is also an indicator of thermal stress [5]. Data points with a mark indicate when first crack in the filter was detected.

SUMMARY/CONCLUSIONS

A next generation of cordierite based diesel particulate filters was introduced addressing future needs of low pressure drop, low thermal mass systems designed for optimized passive regeneration and low thermal inertia for fast heat up of a downstream SCR system, with the overall objective to minimize CO_2 emission.

The new materials are based on a thin wall design with optimized material and microstructure, resulting in an almost linear pressure drop response with soot loading in the bare and catalyzed state. Compared against current EPA 2010 filter technologies, ~40% reduction in pressure drop (same volume) or ~20% reduction in volume (same pressure drop) for the 200/8 design is expected. In addition, inlet volume is ~15% higher for more ash storage capability. For the 300/7 ACT design, similar improvement in pressure drop or volume, and even more improvement in ash storage capability are expected.
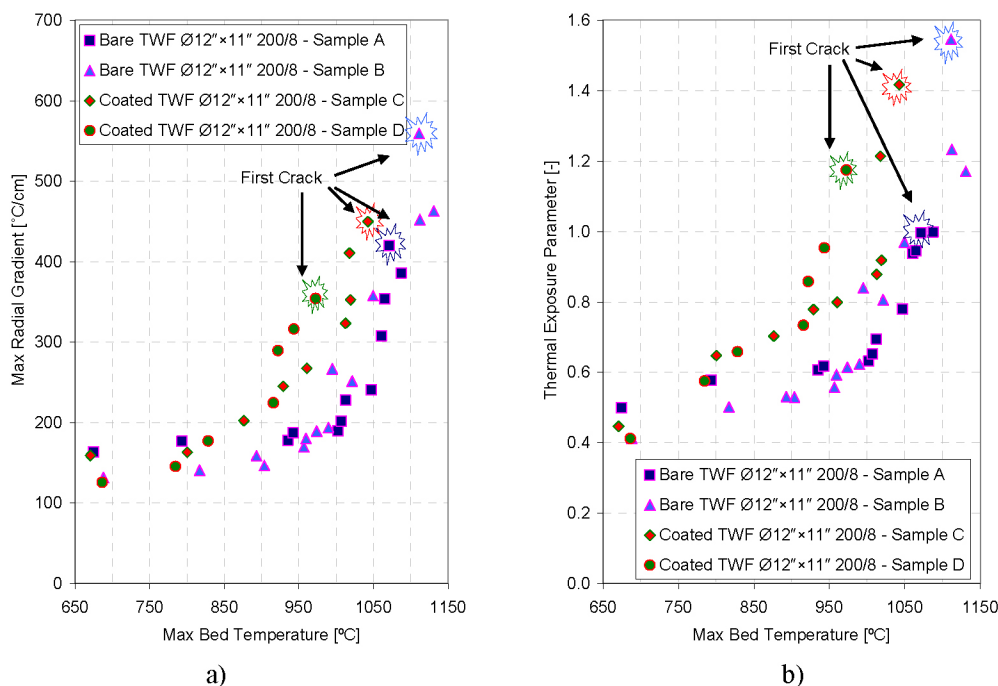
Figure 15. a) Radial gradient and b) thermal exposure parameter as a function of max bed temperature.

The new TWF shows a faster thermal response during cold start due to ~45% less thermal mass and thus enable an extended operating temperature range for filter passive regeneration and downstream SCR deNOx reaction, especially for cold start conditions. During regeneration, when the convective heat removal is sufficient to manage extreme exotherms, the TWF has similar maximum bed and mid bed temperature, while the skin temperature for the TWF is always higher compared to current EPA 2010 filter technologies. Therefore the TWF enables, in general, higher regeneration efficiency and lower thermal stress under these conditions.

The optimized micro structure enables high filtration efficiency for both mass and number, as demonstrated by filtration tests performed following PM and PMP protocols on a heavy duty engine.

REFERENCES

1. Cutler, W.A., Boger, T., Chiffey, A.F., Phillips, P.R. et al., "Performance Aspects of New Catalyzed Diesel Soot Filters Based on Advanced Oxide Filter Materials," SAE Technical Paper 2007-01-1268, 2007, doi:10.4271/2007-01-1268.

2. Young, D.M., Hickman, D.L., Bhatia, G., and Gunasekaran, N., "Ash Storage Concept for Diesel particulate Filters," SAE Technical Paper 2004-01-0948, 2004, doi:10.4271/2004-01-0948.

3. Aravelli, K. and Heibel, A., "Improved Lifetime Pressure Drop Management for Robust Cordierite (RC) Filters with Asymmetric Cell Technology (ACT)," SAE Technical Paper 2007-01-0920, 2007, doi:10.4271/2007-01-0920.

4. Giechaskiel, B., Carriero, M., Martini, G., and Andersson, J., "Heavy Duty Particle Measurement Program (PMP): Exploratory Work for the Definition of the Test Protocol," *SAE Int. J. Engines* **2**(1):1528-1546, 2009, doi:10.4271/2009-01-1767.

5. Ingram-Ogunwumi, R.S., Dong, Q., Murrin, T.A., Bhargava, R.Y. et al., "Performance Evaluations of Aluminum Titanate Diesel particulate Filters," SAE Technical Paper 2007-01-0656, 2007, doi:10.4271/2007-01-0656.

CONTACT INFORMATION

Thorsten Boger
Corning Incorporated, Science & Technology
SP-DV-02-1, Corning, NY 14831

ACKNOWLEDGMENTS

DEFINITIONS/ABBREVIATIONS

AC

Advanced Cordierite

ACT

Asymmetric Cell

DOC

Diesel Oxidation Catalyst

DPF

Diesel particulate Filter

FTP

Federal Test Procedure

GHG

Greenhouse Gas

PM

particulate Matter

PMP

Particle Measurement Programme

PN

Particle Number

SCR

Selective Catalytic Reduction

TC

Thermocouple

TWF

Thin Wall Filter

WHTC

World Harmonized Transient Cycle

SAE *International*